

Functional imaging of gated Tc-99m tetrofosmin study as a simple method to quantify ventricular wall motion

Kenichi NAKAJIMA,* Junichi TAKI,* Toru MATSUYAMA,** Yoshihito KITA,***
Eui-Hyo HWANG* and Norihisa TONAMI*

*Department of Nuclear Medicine, Kanazawa University Hospital

**Second Department of Internal Medicine, Kanazawa University Hospital

***Department of Internal Medicine, Kaga Chuo Hospital

Myocardial perfusion scintigraphy with wall motion analysis is known to enhance accuracy in diagnosing ischemic heart disease. The purpose of this study is to determine the best method to evaluate regional wall motion in a gated planar perfusion study. Planar gated ^{99m}Tc tetrofosmin (GTF) study in two projections was performed after rest-exercise sequence SPECT studies ($n = 29$). To evaluate wall motion, cine-mode display, wall thickening, and inverted tetrofosmin studies including ventricular inner border tracing, segmental wall shortening and functional images were used. The results were compared with gated blood-pool (GBP) study in the same projections. In the GTF study, functional image identified asynergy significantly better than cinematic display. The best correlation between GTF and GBP studies was observed with functional images of phase and amplitude, with complete visual agreement seen in 145 of 168 (86%) segments. With quantitative analysis by means of regions of interest ($n = 280$), a good correlation was observed between GTF and GBP regarding regional amplitude ($r = 0.78$), regional phase ($r = 0.84$), average left ventricular phase ($r = 0.91$) and standard deviation of phase values ($r = 0.90$). The value for the count-based "ejection fraction" derived from inverted GTF showed insufficient correlation to that of the GBP study ($r = 0.69$). Functional imaging with myocardial perfusion imaging is a simple and effective means to evaluate ventricular asynergy. Similar diagnostic criteria to gated blood-pool imaging and comparable diagnostic accuracy are advantages of this approach.

Key words: myocardial perfusion, gated Tc-99m tetrofosmin study, gated blood-pool study, cardiac function

INTRODUCTION

TECHNETIUM-99m (^{99m}Tc) myocardial perfusion imaging agent has been found to be useful in coronary artery disease in evaluating ischemia, area at risk and myocardial viability. Currently both ^{99m}Tc sestamibi and ^{99m}Tc tetrofosmin are used.¹⁻⁹ It is well recognized that wall motion abnormality has also important diagnostic and prognostic value both in nuclear studies and echocardi-

ography.¹⁰ In comparison with a Tl-201 myocardial perfusion study, ^{99m}Tc radiopharmaceutical has advantages regarding the dose administered, higher photon flux and appropriate energy for data acquisition. This enables gated imaging and provides simultaneous assessment of perfusion and wall motion with a single injection.¹¹⁻¹⁵ Gated single-photon emission computed tomography (SPECT) has recently been used.¹⁶⁻²⁰ Although electrocardiography (ECG) gated SPECT acquisition can be performed with up-to-date SPECT equipment the longer acquisition time is preferable to increase the total count in gated images. Moreover, there is as yet no uniform processing method to integrate many gated tomographic slices. The idea of the planar gated perfusion image presented here is not new, but the quantification of left ventricular function by the method has not been estab-

Received October 25, 1996, revision accepted January 20, 1997.

For reprint contact: Kenichi Nakajima, M.D., Department of Nuclear Medicine, Kanazawa University Hospital, 13-1 Takaramachi, Kanazawa 920, JAPAN.

e-mail: nakajima@med.kanazawa-u.ac.jp

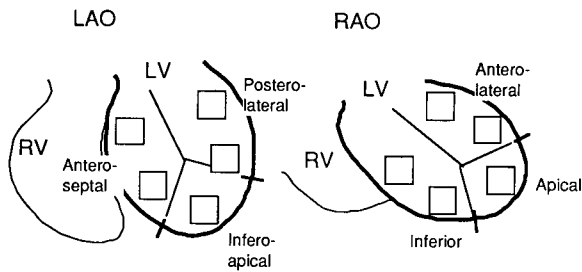


Fig. 1 Regions of gated blood-pool study and gated tetrofosmin study in the LAO and RAO views. In visual interpretation of wall motion, left ventricle was divided into 3 regions for each view. In quantitative analysis, 5 rectangular regions of interest were selected for each view.

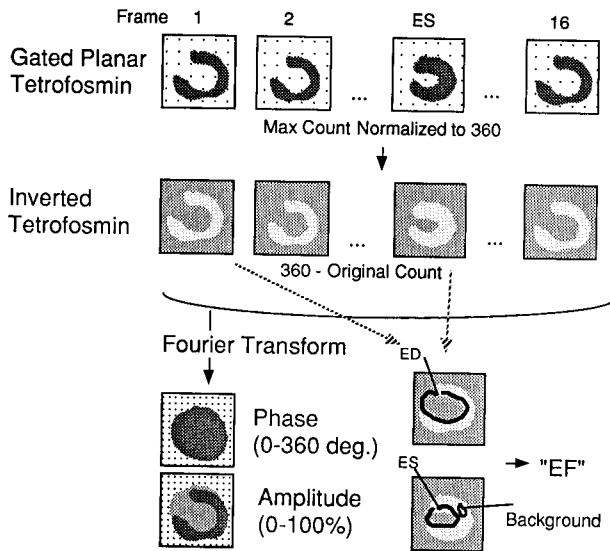


Fig. 2 Planar gated ^{99m}Tc tetrofosmin inversion to make Fourier functional images. Count-based "ejection fraction" was calculated by end-diastolic and end-systolic ventricular count.

lished. Simple means that can be used with ordinary nuclear medicine equipment and processing programs would be convenient and useful. In this study, we proposed functional imaging in multiple projections based on count-inverted images of ^{99m}Tc tetrofosmin and compared with the results of gated blood-pool studies.²¹⁻²³ We evaluated the feasibility of functional images of gated myocardial perfusion scan and its clinical application as in gated radionuclide ventriculography.²⁴⁻²⁸

MATERIALS AND METHODS

Patients

Stress ^{99m}Tc tetrofosmin myocardial scintigraphy was performed in 29 patients aged from 51 years to 80 years (20 males and 9 females, average 64 years, SD 11 years). Eleven patients had old myocardial infarction, 9 acute myocardial infarction, 1 angina pectoris, 4 valvular heart disease, 2 dilated cardiomyopathy, 1 hypertension and diabetes mellitus, and 1 suspected ischemic heart disease.

Percutaneous transluminal coronary angioplasty had been performed in 12 patients, and coronary artery bypass grafting in three. Coronary angiography with cardiac catheterization was performed in 19 patients, and biplane left ventriculography was performed in 10 patients within 7 days of the nuclear study.

^{99m}Tc Tetrofosmin study

In the ^{99m}Tc tetrofosmin study, 250 MBq was injected at rest and 740 MBq was injected at subsequent exercise study. After the second SPECT acquisition, planar gated tetrofosmin (GTF) acquisition was performed with 64×64 matrices, $\times 2$ zoom, and 16 frames per cardiac cycle. The left anterior oblique (LAO) 35 to 45-degree best septal and right anterior oblique (RAO) 10-degree projections were obtained for 5 minutes each.

Gated blood-pool study

Gated blood-pool (GBP) study was performed within 5 days of the tetrofosmin study with 740 MBq of *in vivo* ^{99m}Tc red blood cell labeling. Identical LAO and RAO projection angles were used in the GBP and GTF studies. In 2 patients, only LAO views were obtained. A cardiac cycle was divided into 24 frames with 64×64 matrices. Count loss of the last frames caused by heart rate variation was corrected for both tetrofosmin and gated blood-pool studies.

Analysis of wall motion by gated tetrofosmin study

Cine-mode display. In the visual cine-mode display, the left ventricle was divided into 3 regions, i.e., antero-septal, inferoapical and posterolateral segments in the LAO view, and anterolateral, apical and inferior segments in the RAO view (Fig. 1). The degree of asynergy was visually classified as normokinesis, hypokinesis, severe hypokinesis, akinesis and dyskinesis. Two factors that influence our impression, i.e., movement of the inner edge of myocardium and wall thickening, should be considered.

Wall thickening. Five rectangular regions of interest (ROIs) of 4×4 or 5×5 pixels were set on each myocardial wall in end-diastolic (ED) and end-systolic (ES) frames, and the average count per pixel was calculated. The ROIs were placed in the antero-basal, anterolateral, apical, inferior and basal inferior segments in the RAO projection, and posterolateral, inferolateral, apical, distal septal and basal septal segments in the LAO projection, as in Fig. 1. The background was drawn on the lung along the left ventricle. Wall thickening was defined as (mean ES count - mean ED count) divided by (mean ED count - mean background count).

Inverted tetrofosmin images. The following four methods are based on inverted tetrofosmin images. The method is schematically explained in Fig. 2. The original image was filtered with 9-point weighted spatial smoothing and 3-point 1 : 2 : 1 temporal smoothing. The myocardium

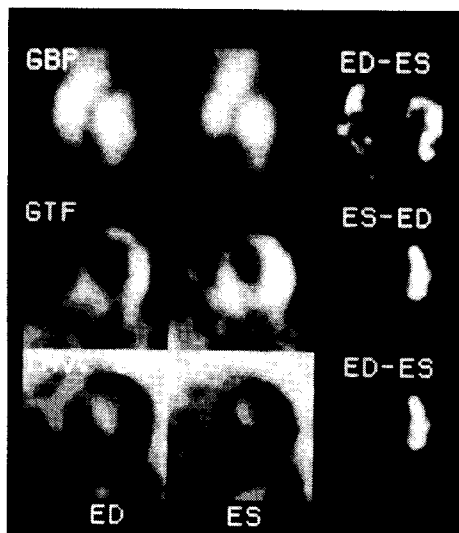


Fig. 3 End-diastolic and end-systolic images of gated blood-pool study (upper), gated tetrofosmin study (middle) and inverted count of gated tetrofosmin (lower). Difference of end-diastolic and end-systolic images, which corresponds to stroke count or changes of wall thickening, is shown on the right. Low count of the anteroseptal region in the LAO view indicates asynergy in this region.

was zoomed ($2\times$) in all patients, and this could usually exclude high hepatic or gall bladder uptake and subphrenic bowel activity. We then determined the maximum count for the myocardial wall and multiplied the constant value so that the myocardial maximum count became 360 counts per pixel. The value of 360 was selected just for displaying phase ($0\text{--}360$ degrees) and myocardial image without scale adjustment. The serial gated images were subtracted from a constant of 360 counts per pixel. The resulting images had high-count pixels in the LV cavity and low values in the myocardial wall, somewhat resembling gated blood-pool images (Fig. 3).

Detection of inner myocardial border. The inner myocardial border was traced by the isocount method, but our preliminary data showed that the constant % threshold was difficult to determine. Myocardial hypertrophy with a relatively small cavity in the ES frame sometimes resulted in variable results.

Shortening of wall motion. Edges determined by the abovementioned method and a center of gravity was used to calculate % radial shortening in 36 segments, but for the same reason, the variation of edges was relatively large and also affected by the location of the left ventricular center.

Functional map of inverted GTF images. A standard program for phase and amplitude images was used.²¹ Phase and amplitude values in each pixel were derived from the fundamental frequency of the discrete Fourier transform. The criteria that have been generally used for

GBP imaging were also applied to GTF imaging. The general pattern of phase and amplitude was visually evaluated as follows. The hypokinetic segment usually shows slightly to moderately reduced amplitude without a delay in phase value. Severe hypokinesis shows markedly reduced amplitude. The akinetic segment shows markedly reduced amplitude or a defect and some of them show slight delay in the phase. The dyskinetic segment is characterized by a significantly delayed phase value with amplitude value depending on the degree of paradox movement. In visual analysis, 3 regions as used in cine-mode evaluation were used. Five 5×5 -pixel rectangular regions of interest were set on the amplitude image corresponding to wall thickening analysis. In phase image, the average left ventricular phase value and its standard deviation were calculated with the LAO view. Regional phase values were calculated as in the amplitude image.

Using inverted tetrofosmin images, a time-activity curve could be generated on the left ventricle. First, an intracavitary blood-pool like image was roughly traced manually, although the basal septum and valve plane were carefully drawn. Subsequently, the isocount of 55–60% of peak ventricular count was used to determine the endocardial border. Further manual modification was necessary in a few cases with noise or a large defect. A background of about 20 pixels was set on the end-systolic inverted myocardial wall including a pixel of the lowest value. With ED and ES counts, a parameter corresponding to the count-based ejection fraction was calculated (EF_{GTF}). Whether this “EF” could be an approximate value for true blood-pool EF was examined. To examine the reproducibility of the results, two operators independently calculated EF_{GTF} , and the same operator repeated the calculation 3 months later.

Analysis of gated blood-pool study

In a visual cine-mode display, the left ventricle was divided into 3 segments as in the GTF study. In the RAO view, posterior or basal septal regions were not evaluated because of overlap of the right ventricular blood pool. The global contractility was evaluated by an ejection fraction (EF_{GBP}) calculation program based on the same threshold method as in the GTF study. After encircling the end-diastolic perimeter manually, an isocount of 60–65% of the maximum ventricular count was used to determine the ROI. In this processing, careful selection was required in the basal septum, valve plane and the border of left atrium and ventricle. This threshold method was automatically repeated in all frames by using the same threshold value. The background was set along the end-diastolic left ventricle from 3 to 6 o'clock. Normal values in our hospital range from 55 to 75%. Functional imaging of phase and amplitude was utilized for evaluating wall motion. In quantitative analysis 5 regions of interest comparable to the GTF study were set on the phase and amplitude

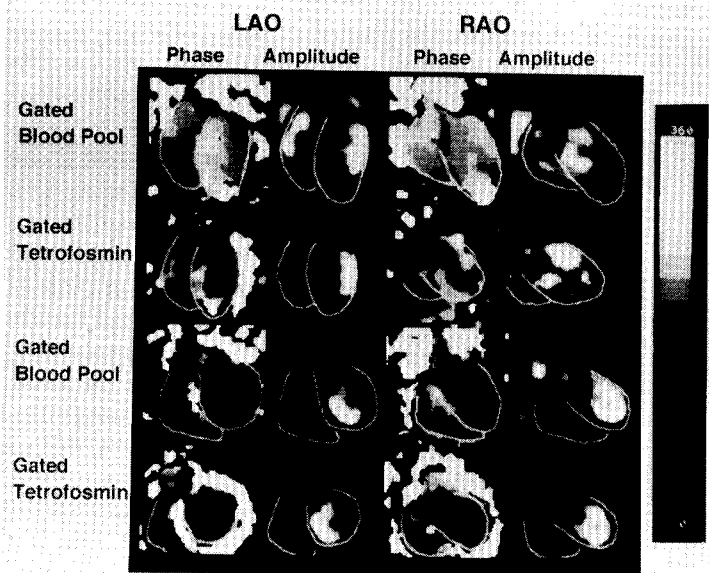


Fig. 4 Upper two panels. Functional images of phase and amplitude in a patient with antero-septal infarction. Phase and amplitude images in the LAO and RAO projections are shown. The larger degree (white) in the phase map indicates more delayed phase, while the high count (white) in the amplitude image indicates good wall motion. Perimeters are manually drawn to identify right and left ventricular edges. Peri-ventricular white color in phase display is probably caused by translation of myocardial walls. The average phase value and SD in the left ventricle were 206 degrees \pm 42 degrees and 191 degrees \pm 37 degrees for gated blood-pool (GBP) and gated tetrofosmin (GTF) studies respectively.

Lower two panels. Functional images in a patient with acute myocardial infarction. Inferior, inferolateral and posterolateral akinesia are observed as reduced amplitude (black color).

Table 1 Comparison of gated blood pool and gated tetrofosmin studies with cine-mode display and functional imaging

A. Cine-mode Display: GBP vs. GTF

		Cine Mode by GTF			Totals
		N	H	A-Dys	
Cine-Mode by GBP	N	92	6	0	98
	H	23	31	1	55
	A-Dys	3	4	8	15
Totals		118	41	9	168

B. GBP study: Functional Image vs. Cine-mode

		Cine Mode by GBP			Totals
		N	H	A-Dys	
Functional Image by GBP	N	74	21	0	95
	H	24	32	4	60
	A-Dys	0	2	11	13
Totals		98	55	15	168

C. GTF study: Cine-mode vs. Functional Image

		Cine Mode by GTF			Totals
		N	H	A-Dys	
Functional Image by GTF	N	82	8	0	90
	H	36	27	2	65
	A-Dys	0	6	7	13
Totals		118	41	9	168

D. Functional Image: GBP vs. GTF

		Functional Image by GTF			Totals
		N	H	A-Dys	
Functional Image by GBP	N	83	12	0	95
	H	7	51	2	60
	A-Dys	0	2	11	13
Totals		90	65	13	168

Statistics	Table			
	A	B	C	D
Complete Agreement	0.78	0.70	0.69	0.86
Chi-square p-value: p<	0.0001	0.0001	0.0001	0.0001
Contingency Coefficient	0.66	0.65	0.61	0.74
Kappa	0.56	0.44	0.41	0.75

GTF, gated tetrofosmin; GBP, gated blood pool
N, normokinesis; H, hypokinesis; A-Dys, akinesia or dyskinesia

images. The average and standard deviation for the whole left ventricle were calculated from the LAO projection.

Statistical analysis

Data are presented as the mean \pm standard deviation (SD). Correlation and linear regression analyses in amplitude, phase and ejection fraction were performed. Student's unpaired T-test was performed to calculate the difference between mean values. Contingency table analysis was performed by comparing two sets of asynergy classifications. Chi-square, p-value, contingency coefficient and kappa coefficient were calculated. A p value <0.05 was considered significant.

RESULTS

Figure 3 illustrates the ideas for inverted gated tetrofosmin images in patients with antero-septal infarction. The ED and ES images from GBP, GTF and inverted GTF are shown. The difference between ED and ES images, the so-called stroke count image is shown on the right. Functional images of phase and amplitude are shown in the upper panel of Fig. 4. The lower panel of Fig. 4 shows a patient with acute myocardial infarction with inferior, inferolateral and posterolateral akinesia.

The GBP and GTF studies with cine-mode display and functional imaging were compared in Tables 1A to D. On comparing cine-mode displays for GBP and GTF (Table 1A), GBP showed 70 segments of asynergy including hypokinesis to dyskinesia, while GTF showed only 50 segments of asynergy. In the GBP study (Table 1B), cine-mode display and functional imaging results showed comparable detectability, but in the GTF study, functional images showed significantly higher diagnostic capability than cine-mode evaluation (Table 1C). Cine-mode display detected 41 hypokinetic segments and 9 akinetic or dyskinetic segments, whereas functional imaging detected 65 hypokinetic regions and 13 akinetic or dyskinetic regions. Functional images of GTF and GBP showed a

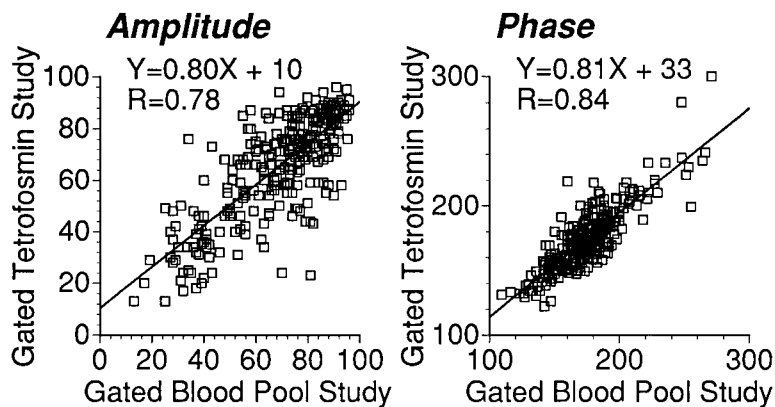


Fig. 5 Correlation of amplitude (left) and phase (right) values between the gated tetrofosmin and blood-pool studies.

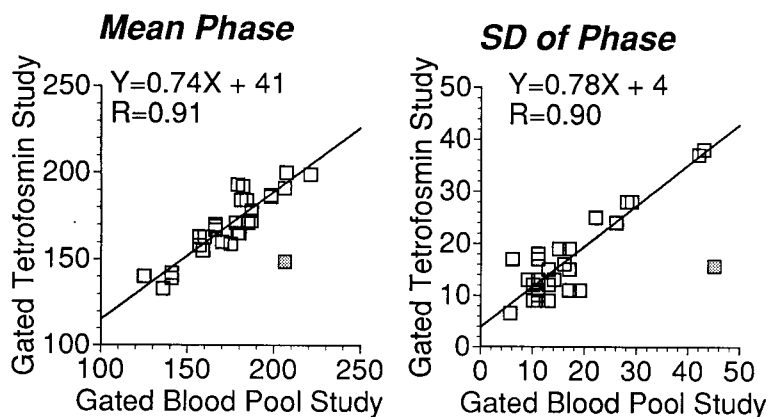


Fig. 6 Correlation of mean phase (left) and standard deviation (right) between the gated tetrofosmin and blood-pool studies. One patient with a large perfusion defect indicated by shaded square was neglected when calculating regression line.

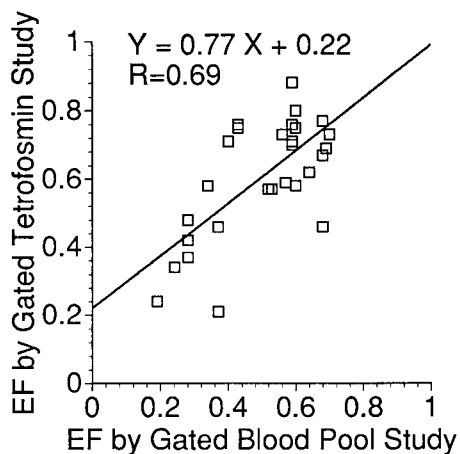


Fig. 7 Correlation of count-based "ejection fraction" between the gated tetrofosmin and blood-pool studies.

high concordance rate (Table 1D), with complete agreement observed in 145 of 168 segments (86%).

When GBP and inverted GTF phase and amplitude patterns were compared, the size of the left ventricular region on the functional map was smaller in the GTF study, as shown in Fig. 4. Peri-ventricular artifacts along the left ventricle were observed in some patients, and were probably caused by a mixture of contraction and translation movement of the myocardium. In some patients, noise was greater in the GTF amplitude map than that in the GBP amplitude map. One patient showed a discrep-

ancy between these studies regarding the phase pattern. The area of apical dyskinesia that was evident in the GBP phase map was small in the GTF phase map. A complete perfusion defect as in this patient could be a cause of discordance.

In quantitative analysis, functional imaging with inverted GTF gave the best correlation with the GBP study. In 280 regions of interest, GTF amplitude (%) had a good correlation with GBP amplitude (%) as shown in Fig. 5: $\text{Amplitude}_{\text{GTF}} = 0.80 \times \text{Amplitude}_{\text{GBP}} + 10$ ($r = 0.78$, $p < 0.0001$). A weak correlation was observed between wall thickening and GBP amplitude ($r = 0.28$, $p < 0.0001$) or GTF ($r = 0.30$, $p < 0.0001$). As for the left ventricular mean phase, except for a patient with large perfusion defect and large phase deviation, GTF and GBP phase values (degree) agreed well, as shown in Fig. 6: $\text{Average Phase}_{\text{GTF}} = 0.74 \times \text{Average Phase}_{\text{GBP}} + 41$ ($r = 0.91$, $p < 0.0001$). Phase SD (degree) of GTF and GBP also showed a good correlation: $\text{SD of Phase}_{\text{GTF}} = 0.78 \times \text{SD of Phase}_{\text{GBP}} + 4$ ($r = 0.90$, $p < 0.0001$). Regional phase values excluding the above mentioned patient with a large defect also showed a good correlation between GBP and GTF studies: $\text{Phase}_{\text{GTF}} = 0.81 \times \text{Phase}_{\text{GBP}} + 33$ ($r = 0.84$, $p < 0.0001$, 270 regions), as shown in Fig. 5.

In 10 patients who underwent left ventriculography, the severity of asynergy was compared to regional amplitude values in the GBP and GTF studies. The maximum amplitude value was normalized to 100 per pixel. In the GBP study, amplitude in normokinesis was 77 ± 12 , while

those in hypokinesis and akinesis/dyskinesis were 64 ± 18 and 51 ± 29 ($p = 0.003$ and 0.0023 respectively vs. normokinesis). In the GTF study, amplitude in normokinesis was 75 ± 11 , while those in hypokinesis and akinesis/dyskinesis were 61 ± 15 and 54 ± 23 ($p < 0.0001$ vs. normokinesis for both).

The count-based "EF" value determined by inverted GTF showed a fair correlation to GBP EF: $EF_{GTF} = 0.77 \times EF_{GBP} + 0.22$ ($r = 0.69$). Although the correlation coefficient was not bad, the variation in EF was relatively large. On the line of $EF_{GBP} = 40\%$, EF_{GTF} ranged from 20 to 80% (Fig. 7), whereas the reproducibility of the processing for the EF_{GTF} was generally good. Interobserver reproducibility was EF (operator 1) = $0.75 \times EF$ (operator 2) + 0.13 ($r = 0.90$, $p < 0.0001$). The intraobserver reproducibility was EF (first) = $0.90 \times EF$ (second) + 0.06 ($r = 0.94$, $p < 0.0001$). The background value including the lowest inverted myocardial count was 23 ± 7 count/pixel corresponding to $6.4\% \pm 2.0\%$ of 360 count/pixel.

DISCUSSION

Simultaneous assessment of perfusion and wall motion

Simultaneous evaluation of wall motion added further information to the perfusion study alone, in increasing diagnostic accuracy, avoiding artifacts and providing some prognostic value.¹²⁻¹⁹ In general, ventricular asynergy is seen in hypoperfused areas and akinesis or dyskinesis in severe perfusion defects. In the acute phase of infarction, particularly after reperfusion, myocardial stunning may be seen as near normal perfusion with reduced wall motion or segmental systolic thickening. Hibernation may be detected as hypokinesis in a hypoperfused area that maintains viability. Functional status as well as perfusion would be important in evaluating these situations.

The TI-201 gated study has also been performed, but is not as well accepted as a routine study. On the other hand, ^{99m}Tc has more appropriate characteristics for gating. Only 5-minute acquisition for a projection was a practical time in addition to SPECT, since many hospitals still use multiple, at least two, planar images in conjunction with SPECT study.

Additional wall motion study may be also useful from the viewpoint of cost-effectiveness, since the number of nuclear studies including perfusion, function and metabolism has increased recently.

Why is planar study used?

Instead of planar imaging, the current trend in myocardial scanning is the SPECT study.²⁹ Although gated perfusion SPECT has been reported to be useful in the diagnosis of cardiac function,¹⁶⁻²⁰ it has not been practical enough for routine use in a busy nuclear medicine department because of the complexity of the processing program. The

result format has not been established, and integration of many SPECT slices requires special programs. Polar map display is an interesting approach, but the correspondence of different ED and ES sizes and reliability of wall thickening analysis require further investigation. Three-dimensional display is also an intriguing approach,²⁰ but whether it enhances the diagnostic ability is not clear. While the diagnostic methods have become complex, planar imaging, on the other hand, is a simpler procedure and needs no special equipment. Although we recognize the usefulness of the gated SPECT, a simpler method may be more readily accepted provided that it is reliable. Since many nuclear medicine departments use both SPECT and additional planar views as a backup or confirming surrounding activity such as liver, bowel and lung activity, this planar acquisition may be replaced by the ECG-gated planar method. If necessary, a non-gated image can be simply obtained by adding gated images.

Since the recent development of computer technology using multiple-headed SPECT has shortened the processing time for gated tomography, routine use of gated SPECT may become an option for wall motion analysis. Considering this trend, the detectability of the gated planar and SPECT approach should be compared.

Comparison of several GTF methods

Both edge detection and radial shortening methods are susceptible to a percentage of threshold, low myocardial uptake and statistical noise. Determination of the cavity center also significantly influenced the results. After preliminary results, we abandoned these methods because of the instability of the results.

Cine-mode display of original GTF is the first step for analyzing wall motion, but since movements of both inner and outer edges as well as wall thickening are visible, experience has been necessary for accurate evaluation. Wackers, et al. reported that analysis of endocardial motion on gated ^{99m}Tc isonitrite imaging led to significant underestimation of regional wall motion abnormality.¹¹ Our results also demonstrated that inner border detection was not stable. We preliminarily tested a differentiation method for edge detection, but it also varied according to the shape and counts in the intracavitary activity. Wall thickening did not have a good correlation with GBP amplitude. This may be a limitation of the planar study in calculating the true wall thickness. In this study, we found that functional images are practical and superior to cine-mode or unstable edge-detection methods. Although we detected more abnormality in segmental wall motion with functional images compared with cine-mode display, a further study compared to the gold standard, other than a gated blood pool study would be desirable.

What does inverted GTF image mean?

Inverted intracavitary activity looks like a blood-pool image, but it need not strictly reflect left ventricular

volume. The edge of the myocardial border may not be accurately determined by planar imaging. A change in wall thickness also affects wall motion. From these points of view, calculated phase and amplitude contain major factors in wall thickening, intracavitary count change and translation of the myocardial wall. But a blood-pool study also contains these factors, although possibly to a lesser degree than a GTF study.²³

Even if Fourier analysis was performed directly with a conventional non-inverted image, the amplitude value would be identical to that of the inverted image, but the most frequent phase value in the ventricle, which corresponds to the peak of the phase histogram, is near values of 360 or 0, resulting in splitting of the ventricular phase on both sides of the display scale. The phase shift and separation make the phase pattern difficult to interpret. On the other hand, with inverted count images, ventricular phase values spread around the mid-portion (approximately 180) of the scale, resulting in a similar pattern to that of blood-pool studies.

Advantages and limitations

An advantage of functional imaging is that we can use the same diagnostic criteria as in a GBP study. Any nuclear medicine physician or cardiologist familiar with phase and amplitude analysis can readily interpret the GTF phase and amplitude maps. Usefulness of Fourier image analysis by means of a gated blood-pool study has been described in coronary artery disease.²⁴⁻²⁷ Brateman, et al. compared the cine display with Fourier imaging by using contrast ventriculography as the gold standard.²⁷ They found rather higher diagnostic accuracy (Fourier 86% versus cine 58%). Although Fourier analysis cannot replace the cine display, it can enhance the reading of radionuclide ventriculograms by calling attention to subtle areas of abnormal wall motion that might have been missed by visual analysis, as Becker reported.²⁸

The high 86% agreement rate between GBP and GTF methods encourages the routine use of functional imaging. The patterns are more intuitive and can be a good method to quantify wall motion. Although we experienced a case with a large perfusion defect and phase discrepancy, the planar image usually has overlap of normal myocardium, and is more convenient for calculating the phase value, which may be different from a complete defect as seen in SPECT image. Another advantage is good reproducibility of functional image processing. The method is essentially operator-independent and only depends on the image processing filter and acquisition conditions. These technical factors would be well controlled by technologists.

Our study demonstrated general concordance between GBP and GTF functional images, but whether more precise quantification is possible should be evaluated by increasing the number of patients. A comparison of gated planar and gated SPECT studies will also be required. A

noisy image resulting from limited counting statistics in a few patients may be overcome by increasing the acquisition time.

Regional amplitude is high in comparison with asynergy assessed by contrast left ventriculography; for example, segments with akinesis/dyskinesis showed an average amplitude of 50-60%. Probably several factors are involved: (1) one or 2 segments of hypokinesis may be masked by overlap of normal segments, (2) since the amplitude is a relative value, the amplitude of severe hypokinesis may be overestimated in diffuse asynergy, and (3) amplitude of the dyskinetic segment is a positive value (not a negative value, though the phase is shifted), which can be a cause of overestimation of the average regional count.

A planar gated study was performed after an exercise tetrofosmin study in this protocol. Since the gated study was performed usually > 45 minutes after the injection, the induced asynergy was considered to be recovered except for cases with severe ischemia, but a reduced myocardial count induced by ischemia may cause a slight underestimation of the amplitude. This problem would be partly solved by an exercise-rest sequence stress protocol.

Is the count-based ejection fraction reliable?

Williams, et al. reported that planar ^{99m}Tc sestamibi inversion could be used for calculating the ejection fraction.¹⁵ Since their results were favorable both in phantom and clinical studies, we also examined the EF calculation. Our threshold technique required an initial manual setting, and correlation was fair ($r = 0.65$). They used center-of-mass, derivative threshold border technique for detecting edges, and a correlation of $r = 0.85$ to left ventriculography was described. For background selection, they did not use background subtraction, whereas we used a small background ROI and averaged the pixels around the minimal point. Although we subtracted a slightly higher background count than in their study, the background was relatively stable and reproducibility of EF was good. Our method may be improved by a more automated refined algorithm, but from the present study we concluded that this GTF-"ejection fraction" can be a rough parameter for contractility, and not sufficient for EF estimation.

CONCLUSION

Functional imaging derived from inverted planar gated tetrofosmin is a simple and rapid procedure that can be readily applied in any hospital. Similar diagnostic criteria to blood-pool imaging can be used for quantification of wall motion. The diagnostic capability for asynergy is comparable to that of gated blood-pool studies.

REFERENCES

1. Brown KA, Altland E, Rowen M. Prognostic value of

- normal technetium-99m-sestamibi cardiac imaging. *J Nucl Med* 35: 554–557, 1994.
2. Van Train K, Garcia EV, Maddahi J, Areeda J, Cooke CD, Kiat H, et al. Multicenter trial validation for quantitative analysis of same-day rest-stress technetium-99m-sestamibi myocardial tomograms. *J Nucl Med* 35: 609–618, 1994.
 3. Udelson JE, Coleman PS, Metherall J, Pandian NG, Gomez AR, Griffith JL, et al. Predicting recovery of severe regional ventricular dysfunction. Comparison of resting scintigraphy with ²⁰¹Tl and ^{99m}Tc-sestamibi. *Circulation* 89: 2552–2561, 1994.
 4. Althoefer C, von Dahl J, Biedermann M, Uebis R, Beilin I, Sheehan F, et al. Significance of defect severity in technetium-99m-MIBI SPECT at rest to assess myocardial viability: comparison with fluorine-18-FDG PET. *J Nucl Med* 35: 569–574, 1994.
 5. Braat SH, Leclercq B, Itti R, Lahiri A, Sridhara B, Rigo P. Myocardial imaging with Tc-99m tetrofosmin: comparison of one-day and two-day protocols. *J Nucl Med* 35: 1581–1585, 1994.
 6. Nakajima K, Taki J, Shuke N, Bunko H, Takata S, Hisada K. Myocardial perfusion imaging and dynamic analysis with technetium-99m tetrofosmin. *J Nucl Med* 34: 1478–1484, 1993.
 7. Rigo P, Leclercq B, Itti R, Lahiri A, Braat S. Technetium-99m-tetrofosmin myocardial imaging: A comparison with thallium-201 and angiography. *J Nucl Med* 35: 587–593, 1994.
 8. Tamaki N, Takahashi N, Kawamoto M, Torizuka T, Tadamura E, Yonekura Y, et al. Myocardial tomography using technetium-99m-tetrofosmin to evaluate coronary artery disease. *J Nucl Med* 35: 594–600, 1994.
 9. Matsunari I, Fujino S, Taki J, Senma J, Aoyama T, Wakasugi T, et al. Myocardial viability assessment with technetium-99m-tetrofosmin and thallium-201 reinjection in coronary artery disease. *J Nucl Med* 36: 1961–1967, 1995.
 10. Smart SC. The clinical utility of echocardiography in the assessment of myocardial viability. *J Nucl Med* 35 (Suppl 1): 49S–58S, 1994.
 11. Wackers F, Mattera J, Bowman L, Zaret B. Gated Tc-99m-isonitrile myocardial perfusion imaging: Disparity between endo-, epicardial wall motion. *Circulation* 76 (S4): 203–207, 1987.
 12. Marcassa C, Marzullo P, Parodi O, Sambuceti G, L'Abbate A. A new method for noninvasive quantitation of segmental myocardial wall thickening using technetium-99m 2-methoxy-isobutyl-isonitrile scintigraphy—results in normal subjects. *J Nucl Med* 31: 173–177, 1990.
 13. Tischler MD, Niggel JB, Battle RW, Fairbank JT, Brown KA. Validation of global and segmental left ventricular contractile function using gated planar technetium-99m sestamibi myocardial perfusion imaging. *J Am Coll Cardiol* 23: 141–145, 1994.
 14. Jamar F, Topcuoglu R, Cauwe F, De Coster P, Roelants V, Beckers C, et al. Exercise gated planar myocardial perfusion imaging using technetium-99m sestamibi for the diagnosis of coronary artery disease: an alternative to exercise tomographic imaging. *Eur J Nucl Med* 22: 40–48, 1995.
 15. Williams KA, Taillon LA. Gated technetium 99m-labeled sestamibi myocardial perfusion image inversion for quantitative scintigraphic assessment of left ventricular function. *J Nucl Cardiol* 2: 285–295, 1995.
 16. Manting F, Manting MGM. Gated SPECT with technetium-99m-sestamibi for assessment of myocardial perfusion abnormalities. *J Nucl Med* 34: 601–608, 1993.
 17. DePuey EG, Rozanski A. Using gated technetium-99m sestamibi SPECT to characterize fixed myocardial defects as infarct or artifact. *J Nucl Med* 36: 952–955, 1995.
 18. DePuey EG, Nichols K, Dobrinsky C. Left ventricular ejection fraction assessed from gated technetium-99m-sestamibi SPECT. *J Nucl Med* 34: 1871–1876, 1993.
 19. Williams KA, Taillon LA. Left ventricular function in patients with coronary artery disease assessed by gated tomographic myocardial perfusion images. *J Am Coll Cardiol* 27: 173–181, 1996.
 20. Faber TL, Akers MS, Peshock RM, Corbett JR. Three-dimensional motion and perfusion quantification in gated single-photon emission computed tomograms. *J Nucl Med* 32: 2311–2371, 1991.
 21. Adams WE, Tarcowska A, Bitter F. Equilibrium (gated) radionuclide ventriculography. *Cardiovasc Radiol* 2: 161–173, 1979.
 22. Links JM, Douglass KH, Wagner HN Jr. Patterns of ventricular emptying by Fourier analysis of gated blood-pool studies. *J Nucl Med* 21: 978–982, 1980.
 23. Wendt RE III, Murphy PH, Clark JW Jr, Burdine JA. Interpretation of multi-gated Fourier functional images. *J Nucl Med* 23: 715–724, 1982.
 24. Walton S, Yiannikas J, Jarritt PH, Brown NJG, Swanton RH, Ell PJ. Phasic abnormalities of left ventricular emptying in coronary artery disease. *Br Heart J* 46: 245–253, 1981.
 25. Turner DA, Shima MA, Ruggie N, Von Behren PL, Jrosky MJ, Ali A, et al. Coronary artery disease: detection by phase analysis rest/exercise radionuclide angiocardiograms. *Radiology* 148: 539–545, 1983.
 26. Henze E, Tymiec A, Delagardelle C, Adam WE, Bitter F, Stauch M. Specification of regional wall motion abnormalities by phase analysis of radionuclide angiograms in coronary artery disease and non-coronary artery disease patients. *J Nucl Med* 27: 781–787, 1986.
 27. Brateman L, Buckley K, Keim SG, Wargovich T, Williams CM. Left ventricular regional wall motion assessment by radionuclide ventriculography: A comparison of cine display with Fourier imaging. *J Nucl Med* 32: 777–782, 1991.
 28. Becker LC. [Editorial] Radionuclide ventriculography: Should Fourier analysis replace the cine display. *J Nucl Med* 32: 782–784, 1991.
 29. Fintel DJ, Links JM, Bricker JA, Frank TL, Parker M, Becker LC. Improved diagnostic performance of exercise thallium-201 single photon emission tomography over planar imaging in the diagnosis of coronary artery disease. A receiver operating characteristic analysis. *J Am Coll Cardiol* 13: 600–612, 1989.